Materials Science and Engineering C 68 (2016) 585–593

Contents lists available at ScienceDirect

Materials Science and Engineering C

journal homepage: www.elsevier.com/locate/msec

A label-free aptasensor based on polyethyleneimine wrapped carbon nanotubes in situ formed gold nanoparticles as signal probe for highly sensitive detection of dopamine

Azadeh Azadbakht [a,*], Mahmoud Roushani [b], Amir Reza Abbasi [a], Saeid Menati [a], Zohreh Derikvand [a]

[a] Department of Chemistry, Khorramabad Branch, Islamic Azad University, Khorramabad, Iran
[b] Department of Chemistry, Ilam University, Ilam, Iran

ARTICLE INFO

Article history:
Received 1 February 2016
Received in revised form 10 April 2016
Accepted 18 May 2016
Available online 20 May 2016

Keywords:
Aptasensor
Polyethyleneimine
Gold nanoparticles
Dopamine

ABSTRACT

Herein, a highly sensitive and selective aptamer biosensor for quantitative detection of a model target, dopamine (DA), was developed by using a gold (Au) electrode modified with highly dispersed gold nanoparticles (AuNPs) and acid-oxidized carbon nanotubes (CNTs-COOH) functionalized with polyethyleneimine (PEI). Amine-terminated12-mercaptureprobe (ssDNA1) as a capture probe and specific DA-aptamer (ssDNA2) as a detection probe was immobilized on the surface of a modified electrode via the formation of covalent amide bond and hybridization, respectively. Methylene blue (MB) was used as the redox probe, which was intercalated into the aptamer through the specific interaction with its guanine bases. In the presence of DA, the interaction between aptamer and DA displaced the MB from the electrode surface, rendering a lowered electrochemical signal attributed to decreased amount of adsorbed MB. The developed electrochemical DA aptasensor showed a good linear response to DA from 5 to 300 nM with detection limit of 2.1 nM. The biosensor also exhibited satisfactory selectivity and could be successfully used to detect DA in blood serum sample.

1. Introduction

Aptamers are synthetic DNA or RNA sequences that are selected through SELEX (systematic evolution of ligands by exponential enrichment) processes from a random sequence bank [1,2]. High affinity and specific binding usually occur between a selected aptamer and its related target molecule. The combination of good binding affinity and excellent selectivity makes aptamers as attractive as antibodies when used as critical identification materials during protein analysis. Aptamers are, however, more stable, easier to store, and cheaper than antibodies. Furthermore, aptamers can be synthesized without using a host. Therefore, aptamers have been used as alternatives to antibodies in various fields for various applications [3–6]. Variety of aptasensors have been developed using different analytical methods including optical transduction [7], circular dichroism [8], electrochemical techniques [9], fluorimetry [10], colorimetry [11], atomic force microscopy (AFM) [12], surface plasmon resonance (SPR) [13], and quartz crystal microbalance (QCM) [9]. Among these methods, electrochemical aptasensors have attracted particular attention because of the merits of fast response, high sensitivity, simple operation, miniaturization and relatively low cost [14–16].

Dopamine (DA) is one of the most significant catecholamine, belongs to the family of excitatory chemical neurotransmitter. It controls many biological functions such as emotion, endocrine regulation, motivation, locomotion, and so on. Furthermore, some diseases such as Parkinson, schizophrenia and Huntington's chorea are linked to extreme abnormalities of DA levels [17–19]. Therefore, the development of methods for the highly selective and portable determination of DA is of significant importance and is the subject of constantly analytical chemical research. Toward this goal, many researchers have been attracted to work on the determination of DA [20,21]. DA aptamer was discovered in recently [22]. And some methods based on the aptamer technology were developed [23–25]. Although these methods have made great contributions to the determination of DA, each of these approaches exhibits some features that limit practical use, such as the cross-sensitivity toward other chemicals, and the sophisticated detection methods. Thus, the development of a simple and highly sensitive aptasensor with low cost for measurement of DA remains a great challenge.

In the present study, the *AuNPs/PEI/CNTs-COOH* nanocomposite was used as a sensing platform for immobilization of DA-aptamer. MB was chosen as the electrochemical indicator because of its specific binding to dsDNA. The fabrication of the aptasensor was based on the covalent attachment of amine-terminated capture probe on to the nanocomposite by covalent amide bonds formed between the carboxyl groups on

* Corresponding author.
E-mail address: Azadbakht.a@gmail.com (A. Azadbakht).

http://dx.doi.org/10.1016/j.msec.2016.05.077
0928-4931/

the nanotubes and the amino groups on the oligonucleotides. Immobilization of the DA-specific aptamer on the surface of *AuNPs/PEI/CNTs-COOH* was occurred through its hybridization with the capture probe. In the presence of DA, the MB peak current decreased due to formation of a complex between the aptamer and DA and desorption of intercalated MB from the electrode surface.

2. Experimental

2.1. Chemicals

Multiwall carbon nanotubes with purity 95% (10–20 nm diameters) and 1 μm length were obtained from Nanolab (Brighton, MA). Polyethylenimine (PEI, branched, Mw 10,000) ,hydrochloric acid (37%), potassium ferricyanide ($K_3Fe(CN)_6$), potassium ferrocyanide ($K_4Fe(CN)_6 \cdot 4H_2O$), hydrogen tetrachloroaurate ($HAuCl_4 \cdot 4H_2O$) and potassium chloride (KCl) were purchased from Merck (Germany) and Fluka. The sequence of 3′-amine-terminated capture probe containing12 bases was (3′-NH_2-$(CH_2)_6$-CAG AGA CAC ACG-5′) and sequence of aptamer probe containing 58 bases was (5′-GTC TCT GTG TGC GCC AGA GAA CAC TGG GGC AGA TAT GGG CCA GCA CAG AAT GAG GCC C-3′). This sequence was designed to hybridize with the 12-base capture probe and specifically recognize DA. *N*-hydroxysuccinimide (NHS) and 1-ethyl-3-(3-dimethylaminopropyl) carbodiimide hydrochloride (EDC) were produced by Sigma and used as received without further purification. All other chemicals were of analytical reagent grade and used without further purification. Solutions were deaerated by bubbling high purity (99.99%) of nitrogen gas through them prior to the experiments. All experiments were carried out at ambient temperature of 25 ± 1 °C. Cyclic voltammetry (CV), electrochemical impedance spectroscopy (EIS), and differential pulse voltammetry (DPV) were recorded to study the fabrication of modified electrode.

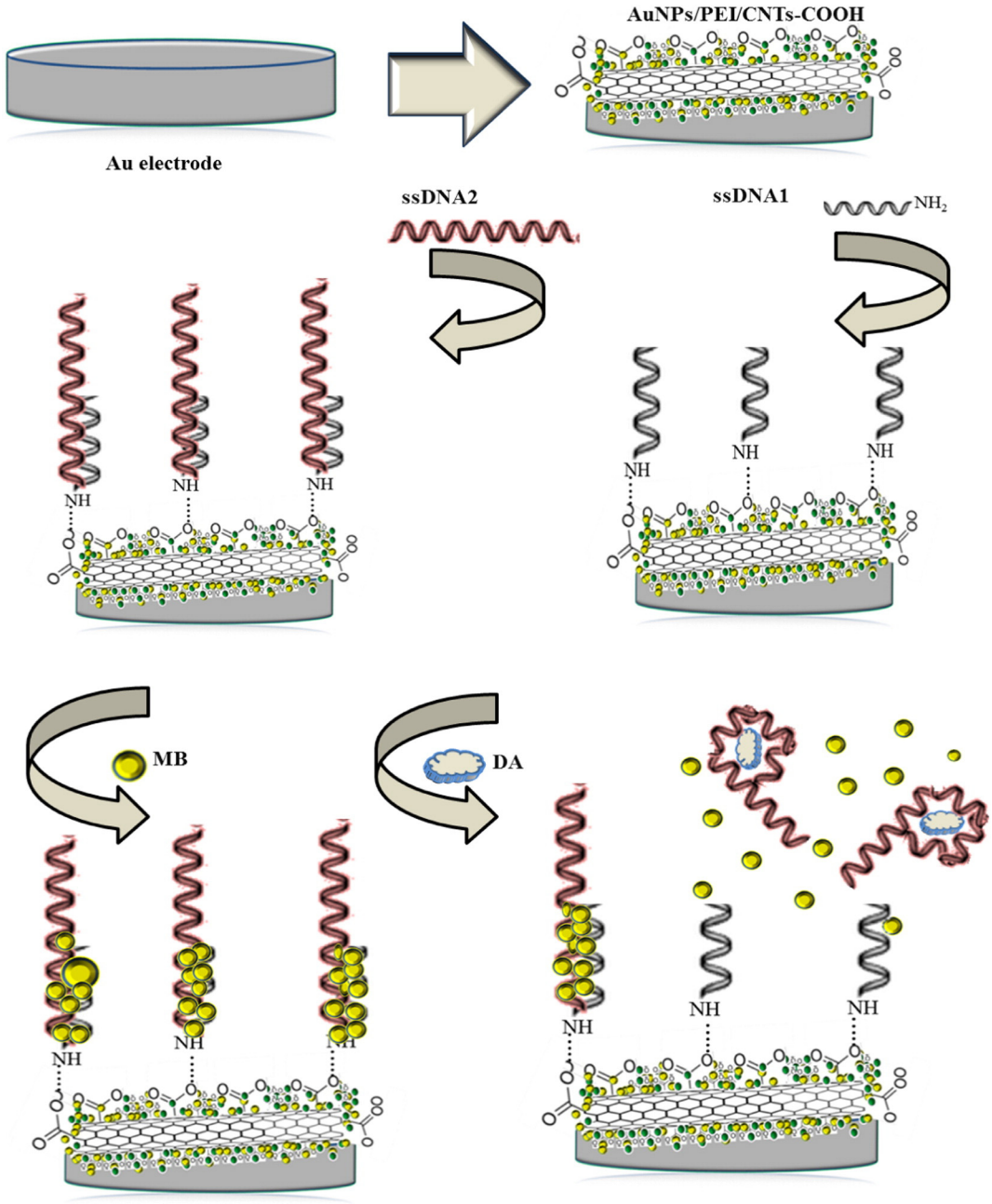

Scheme 1. Schematic representation of different steps of aptasensor fabrication.

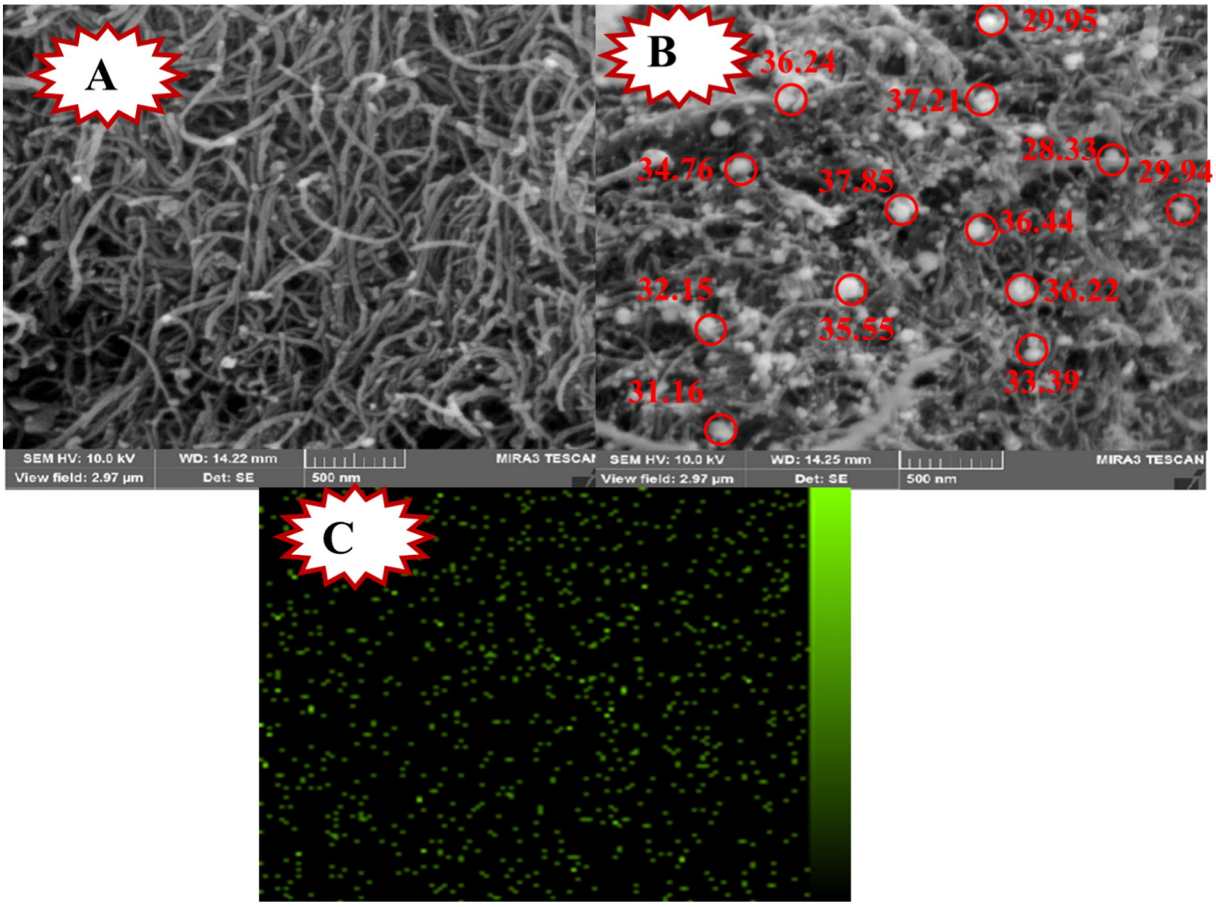

Fig. 1. Typical SEM image of Au/CNTs-COOH (A) and Au/AuNPs/PEI/CNTs-COOH (B) electrodes. (C) wavelength-dispersive X-ray analysis for AuNPs.

2.2. Apparatus

Electrochemical experiments were performed via using a μAutolab III (Eco Chemie B.V.) potentiostat/galvanostat by NOVA 1.8 software. A conventional three electrode cell was used with an Ag/AgCl electrode (KCl 3 M) as the reference electrode, a Pt wire as counter electrode and a modified Au electrode as working electrode. The cell was a one compartment cell with an internal volume of 10 mL. JENWAY pH meter (model 3345) was also applied for pH measurements. To obtain information about the morphology and size of the particles, scanning electron microscopy (SEM) was performed using an X-30 Philips instrument. Wavelength-dispersive X-ray (WDX) was taken on a Vega-Tescan electron microscope. Also, Fourier transform infrared (FT-IR) and UV–vis spectrums were recorded by an AVATAR-370 Fourier transform infrared spectroscopy and a Unico 2800 UV/vis spectrophotometer, respectively.

2.3. The preparation of AuNPs/PEI/CNTs-COOH composite

CNTs were purified by refluxing in 3 M nitric acid for 12 h in the temperature of 150 °C. After subsiding, the sediments were washed with double deionized water. The suspension was filtered and subsequently dried on the temperature of 60 °C. The resultant solid was sonicated in the mixed solution of HNO_3 and H_2SO_4 (1:3, v/v) for 3 h. In order to obtain acid-oxidized carbon nanotubes (CNTs-COOH), the pH of the mentioned solution was adjusted to 8.0 using NaOH (15%).

The preparation of the nanocomposite was according to the literature [26,27]. Briefly, 3.4 mg of CNTs-COOH was distributed in 10 mL double deionized water. Subsequently, 0.7 mL PEI aqueous solution and 2 mL $HAuCl_4$ (18 mM) were added to it and the mixture was taken in 70 °C water bath for 2 h to reduce $HAuCl_4$ to AuNPs. Next, 1.5 mL double deionized water was added to the precipitation to obtain the sensing nanocomposite of AuNPs/PEI/CNTs-COOH.

Cationic PEI was coated onto CNTs-COOH by virtue of electrostatic interaction. More importantly, it has been reported that amines possess high affinity for physisorption along the CNTs-COOHs' sidewalls. So, the driving force involved in the functionalization of PEI on CNTs-COOHs' sidewalls was a combination of the electrostatic interaction between the oppositely charged CNTs-COOH and the PEI and the physisorption process which is analogous to the polymer wrapping process [26–28]. The high density of imino-groups on PEI played an important role in the adsorption of anionic $AuCl_4^-$ followed by reducing of $AuCl_4^-$.

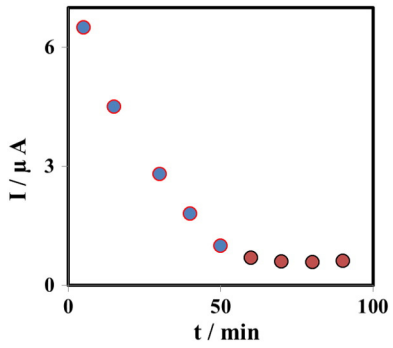

Fig. 2. Effects of DA incubation time on the current response of the modified electrode in the presence of DA using various incubation times.

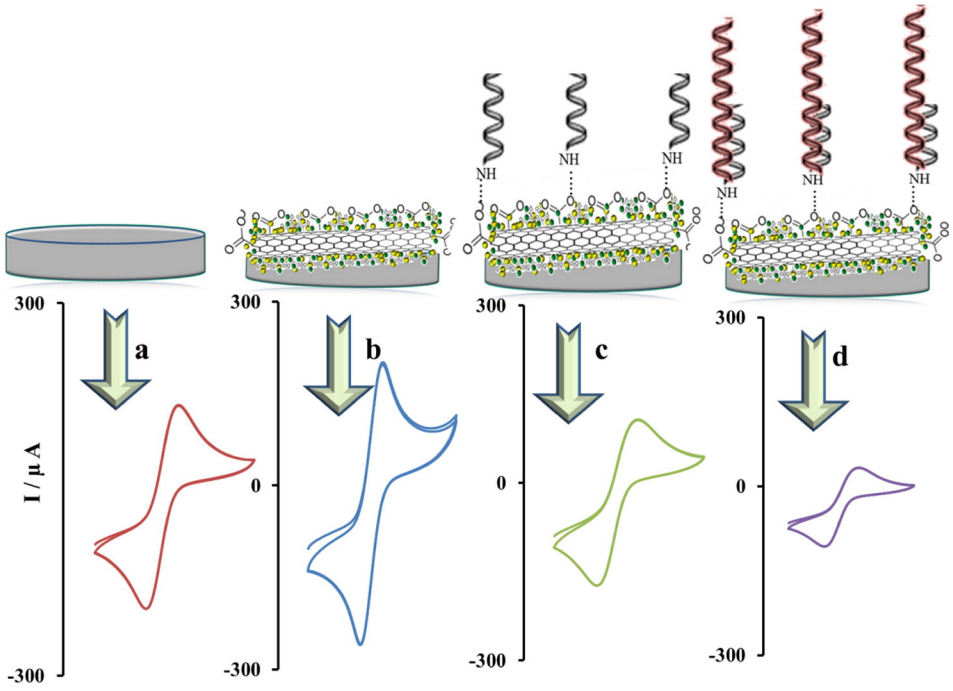

Fig. 3. CVs for bare Au (curve a), Au/AuNPs/PEI/CNTs-COOH (curve b), Au/AuNPs/PEI/CNTs-COOH/ssDNA1 (curve c) and Au/AuNPs/PEI/CNTs-COOH/ssDNA1/ssDNA2 (curve d) electrodes recorded in 0.1 M PBS solution containing 0.5 mM $Fe(CN)_6^{3-/4-}$ at a scan rate of 50 mV s^{-1}.

2.4. Electrode modification

The working electrode was an Au disk electrode with a diameter of 3 mm. Prior to each treatment, the Au working electrode (Metrohm) was polished with alumina slurry down to 0.05 mm on a polishing cloth followed by sonication in distilled water and absolute ethanol. Then the Au electrode was electrochemically cleaned by cycling the electrode potential between −0.4 and 1.2 V vs. Ag/AgCl electrode in 0.5 M H_2SO_4 at a scan rate of 100 mV s^{-1} until the CV characteristics for a clean Au electrode were obtained. Then, 10 μL of AuNPs/PEI/CNTs-COOH solution was cast on the surface of Au electrode and dried in air to form a film at electrode surface. Afterward, the electrode was thoroughly rinsed with water and kept at room temperature for further use.

The nanocomposite could adhere on the surface of gold electrode strongly due to the good ability to form film of the polyelectrolyte and strong adsorbility of AuNPs. Furthermore, the use of polymers as anchors for CNTs has been justified [29–31]. Concerning the CNTs-COOH interaction to PEI, when the electrode was prepared without PEI film, there was not a stable CNTs-COOH binding to the electrode surface.

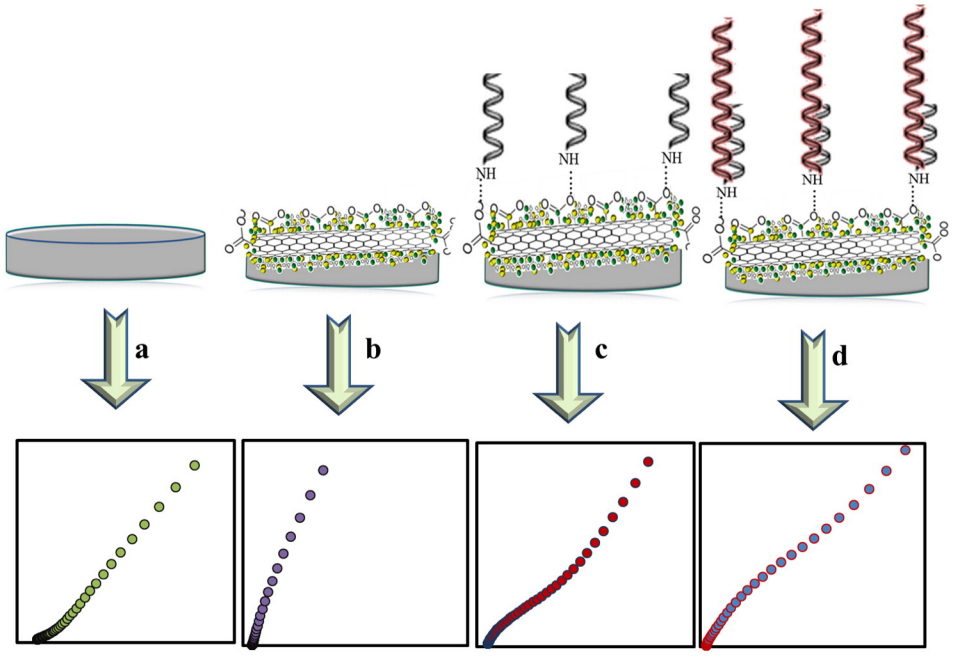

Fig. 4. Nyquist plots for bare Au (curve a), Au/AuNPs/PEI/CNTs-COOH (curve b), Au/AuNPs/PEI/CNTs-COOH/ssDNA1 (curve c) and Au/AuNPs/PEI/CNTs-COOH/ssDNA1/ssDNA2 (curve d) electrodes recorded in 0.1 M PBS solution containing 0.5 mM $Fe(CN)_6^{3-/4-}$ in the frequency range of 10 kHz–0.1 Hz.

For oligonucleotide immobilization, 10 μL of 20 μM 3′-amine capture probe (ssDNA1) containing 10 mM EDC and NHS was dropped on the surface of the modified electrode and the electrode was kept for 2 h at 4 °C. In this process the probe oligonucleotides were immobilized on the Au electrode through the covalent amide bonds formed by the carboxyl groups on the nanotubes and the amino groups on the oligonucleotides.

After rinsing with water, 10 μL of 20 μM 58-base DA aptamer (ssDNA2) was added and incubated on the prepared electrode for 5 h at 4 °C to hybridize with the ssDNA1 as illustrated in Scheme 1. Afterwards, MB was accumulated on to the aptamer-modified electrode surface by dropping 5 μL of MB (20 μM) in Tris–HCl (10 mM Tris-HCl, pH 7.4, containing $CaCl_2$, KCl, NaCl, and EDTA) solution at a ratio of 1:1 for 60 min. Finally, this electrode was thoroughly rinsed with high ionic strength rinsing buffer.

The obtained Au electrode modified with AuNPs/PEI/CNTs-COOH/ssDNA1/ssDNA2/MB is denoted as Au/AuNPs/PEI/CNTs-COOH/aptamer/MB. For determination of DA, 10 mL DA solutions in different concentrations were incubated onto the sensing surface. After 1 h, the electrode was rinsed with rinsing buffer to remove nonspecific adsorption of DA. The peak current of accumulated MB was measured as a function of the DA concentration. The electrochemical characterization of the modified electrode after each step of modification was performed using EIS, CV and DPV techniques.

3. Results and discussion

3.1. Characterization of the modified electrode by SEM

Fig. 1 shows the SEM images of the CNTs–COOH (A) and AuNPs/PEI/CNTs–COOH (B). As can be seen from Fig. 1B, the gold nanoparticles are anchored around the sidewalls of the CNT–COOH, which agree with the results published in the literature [26]. The proper formation of homogeneous nanocomposite suggests that CNTs–COOH and AuNPs may have been uniformly integrated with PEI. AuNPs with average diameter of 31 nm and spherical form dispersedly adhere to the sidewalls of CNTs–COOH. One of the advantages of the present study is the use of AuNPs with small size. So, there would be a strong interaction between the nanoparticles and other modified materials. To further confirm the presence of AuNPs on the surface of electrode, WDX analysis for AuNPs was taken and the distribution of AuNPs shown in Fig. 1C.

The chemical structure of AuNPs/PEI/CNTs-COOH nanocomposites was identified with Fourier transformation infrared spectroscopy (FITR). As can be seen from Fig. S1, characteristic peaks at 2963, 1643, and 1521 were recorded for AuNPs/PEI/CNTs-COOH nanocomposites which assigned to C—H stretching, C═O stretching and N—H bending, respectively. In addition, the C—N stretching vibration was detected at 1249, 1184 and 1037 cm^{-1}. As illustrated, the O—H region (3400 cm^{-1}) for the CNTs-COOH spectrum overlaps with the amine signals of the PEI (3240 cm^{-1}). The UV–visible spectra of nanocomposite was also taken (Fig.S2). The UV–visible spectra showed characteristic absorption bands at about 530 nm corresponding to the absorption bands of AuNPs, confirming the successful deposition of AuNPs in nanocomposite.

3.2. Optimization of measurement conditions

In order to optimize the analytical performance of the proposed aptasensor, some of the experimental parameters such as linking time between ssDNA1 and CNTs–COOH, hybridization and incubation time were investigated. The optimum interaction time between ssDNA1 and CNTs–COOH for formation of amide coupling, was found to be 2 h. Thus, 2 h was chosen as optimum linking time. Also, the efficiency of hybridization is a key factor in the success of the fabrication of an efficient aptasensor. Through the experiments, the optimum hybridization time between ssDNA1 and ssDNA2 was found to be 5 h.

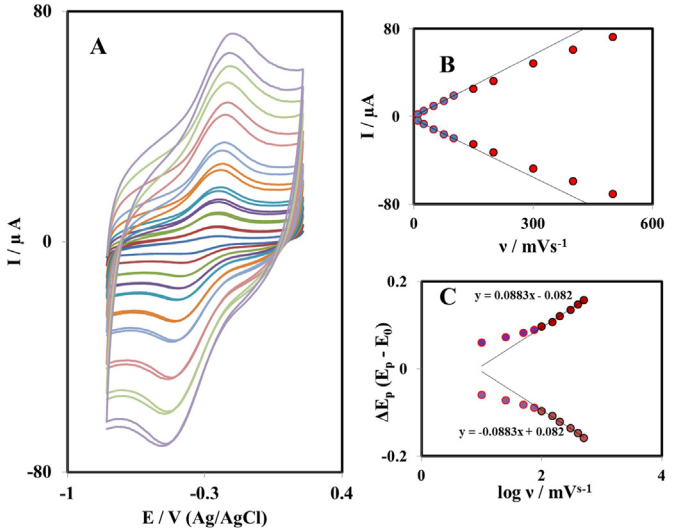

Fig. 5. (A) CVs of Au/AuNPs/PEI/CNTs-COOH/aptamer/MB modified electrode in 0.1 M PBS (pH 7.0) at different scan rates: 10, 25, 50, 75, 100, 150, 200, 300, 400 and 500 mV s^{-1}. (B) Plot of peak currents vs. scan rate. (C) Plot (E_p-E°′) (mV) vs. log *v*.

Furthermore, the effect of DA incubation time on the current response of the sensor was also monitored by recording the peak current response of the modified electrode in the presence of DA using various incubation times. As illustrated from Fig. 2, the current response decreased rapidly with increasing incubation time. The response of modified electrode deviated from the linearity and started to level off for incubation time above 1 h. This result indicated that the formation of aptamer-DA complex was complete after 1 h. Thus, 1 h was chosen as the DA incubation time between the aptamer and DA.

3.3. Detection mechanism of aptasensor

In the absence of DA, MB bound to the aptamer produced a strong DPV signal. But in the presence of DA, the intercalated MB released from the aptamer, resulting an obviously decreased DPV signal. This phenomenon can be applied for DA detection. The redox current of MB was measured to determine the different concentration of DA in the sample. When the aptamer captured DA, the MB-anchored aptamer was desorbed from the surface of electrode; consequently, the significant decrease in the peak current of MB was observed. On the other hand, the peak current of MB decreased linearly with increasing DA concentration due to the formation of aptamer-DA complex and desorption of the MB from the modified electrode surface.

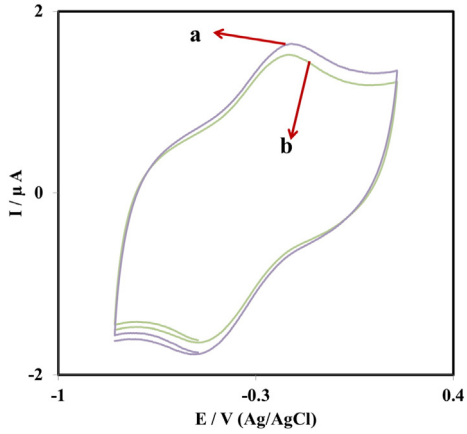

Fig. 6. Recorded CVs for Au/AuNPs/PEI/CNTs-COOH/aptamer/MB in 0.1 M PBS (pH 7.0) before (curve a) and after (curve b) incubation in 50 nM of DA at a scan rate of 50 mV s^{-1}.

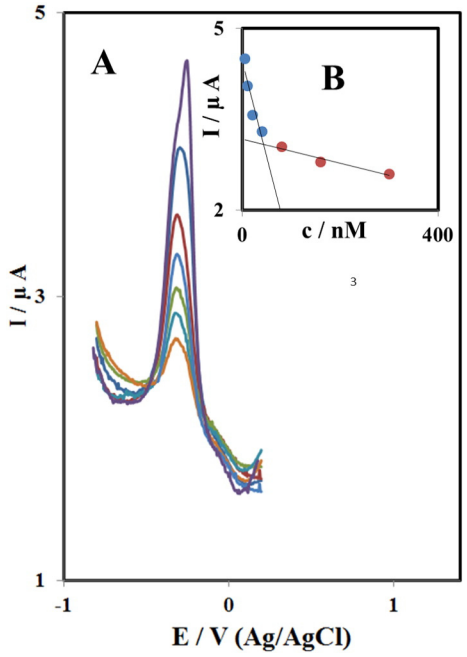

Fig. 7. (A) DPVs obtained for prepared aptasensor recorded in 0.1 M PBS (pH 7.0) after incubation with different concentration of DA: 5 nM, 10 nM, 20 nM, 40 nM, 80 nM, 160 nM, and 300 nM. (B) Plots of reduction peak current of MB vs. DA concentrations.

3.4. Electrochemical behavior of modified electrode

The aptasensor fabrication process was investigated by recording CVs of the modified electrode in 0.1 M phosphate buffer solution (PBS) solution containing 0.5 mM $Fe(CN)_6^{3-/4-}$ during preparation steps (Fig. 3). The CV of $[Fe(CN)6]^{3-/4-}$ was chosen as a marker to investigate the changes of the electrode behavior before and after each assembly step. As it is obvious from Fig. 3, there was reversible redox response for bare Au electrode in the present of $[Fe(CN)6]^{3-/4-}$ (curve a), while for AuNPs/PEI/CNTs-COOH modified electrode, the peak current increased greatly due to increasing effective surface area in the presence of the AuNPs/PEI/CNTs-COOH nanocomposite (curve b). In fact, AuNPs/PEI/CNTs-COOH nanocomposite provided a large effective surface area. However, when ssDNA1 was immobilized at the surface of this electrode, the corresponding CV (curve c), showed a decrease in current response and an increase in the peak-to-peak separation between the cathodic and anodic waves of the redox probe, indicating that the electron-transfer of $[Fe(CN)6]^{3-/4-}$ was obstructed. This result indicated that the covalent attachment of ssDNA1 decreased the conductivity of the electrode surface and reduced available active sites for electron transfer process of $[Fe(CN)6]^{3-/4-}$. Afterward, when 58-mer DA-specific aptamer (ssDNA2) was attached to the surface of the electrode to form AuNPs/PEI/CNTs-COOH/ssDNA1/ssDNA2, the current response of the probe was further decreased (curve d), demonstrating that the ssDNA2 was successfully assembled on the surface.

EIS technique has also been proved to be an effective method for probing the features of surface modified electrodes. Fig.4 shows the typical Nyquist plots for bare Au (curve a), Au/AuNPs/PEI/CNTs-COOH (curve b), Au/AuNPs/PEI/CNTs-COOH/ssDNA1 (curve c) and Au/AuNPs/PEI/CNTs-COOH/ ssDNA1/ssDNA2 (curve d) electrodes recorded in 0.1 M PBS solution containing 0.5 mM $Fe(CN)_6^{3-/4-}$ as an electrochemical redox marker. The straight line at low frequency is related to the diffusion process known as Warburg element, while the high frequency semicircle is related to the electron transfer resistance (R_{ct}), which controls the electron transfer kinetics of the redox probe at the electrode interface. The EIS at a bare Au electrode displayed a very small semicircle and the charge transfer resistance, which was a characteristic feature of the diffusion controlled electrochemical processes (curve a). When AuNPs/PEI/CNTs-COOH was cast at the surface of Au electrode the value of R_{ct} was significantly decreased compared with Au electrode (curve b).

Therefore, immobilization of AuNPs/PEI/CNTs-COOH at the surface of Au electrode facilitates the electron transfer of the redox probe on the modified electrode. After modification of Au/AuNPs/PEI/CNTs-COOH with ssDNA1, the value of R_{ct} was significantly increased (curve c). It indicated hindrance to the electron transfer, confirming the successful immobilization of ssDNA1 onto Au/AuNPs/PEI/CNTs-COOH electrode surface. For the Au/AuNPs/PEI/CNTs-COOH/ssDNA1/ssDNA2 modified electrode, the R_{ct} of the probe was further increased (curve d), which confirmed that the ssDNA2 has been successfully attached to the electrode surface (curve d). The results obtained from the EIS measurements, which are consistent with those from the CVs measurements, clearly confirmed the presence of the immobilized aptamer on the surface of the Au/AuNPs/PEI/CNTs-COOH electrode.

Fig. 5A exhibits the recorded CVs of Au/AuNPs/PEI/CNTs-COOH/aptamer/MB film in 0.1 M PBS at different scan rates. As illustrated, a well-defined redox couple with $E^{\circ\prime} = -0.32$ V (vs. Ag/AgCl) was observed corresponding to the intercalated MB. In Fig. 5B, the plots of anodic and cathodic peak currents vs. the scan rate were presented for the modified electrode. As it is obvious, both the anodic and cathodic peak currents were linearly proportional to the scan rate in the range of 10–100 mV s^{-1}, indicating a surface confined electrode process. The peak-to-peak potential separation was about 112 mV at scan rates below 100 mV s^{-1}, suggesting facile charge transfer kinetics over these range of sweep rates. At higher sweep rates, peak separations began to increase, indicating the limitation due to charge transfer kinetics. The shifts of peak potentials were proportional to the logarithm of the scan rate for scan rates higher than 100 mV s^{-1} (Fig. 5C).

Based on Laviron theory [32], the electron transfer rate constant (k_s) and charge transfer coefficient (α) can be determined. By measuring the

Table 1
Comparison between this method and other reported techniques for detection of dopamine.

Electrode	Electrochemical technique	Detection limit	Linear range	Ref.
Graphene oxide/gold nanoparticle/EDTA sensor probe	–	5.00 nM	10.0 nM–1.00 μM	[33]
Fe_6 complex modified Au electrode	–	0.07 μM	0.20–30.0 μM	[34]
Polypyrrole and graphene modified electrodes	DPV	0.023 μM	0.10–150 μM	[35]
Multilayered hollow microspheres modified electrode	CV	–	500–2000 μM	[36]
carbon nanotube/Nafion modified carbon tape electrode	DPV	10.0 nM	10.0 nM–1.00 μM	[37]
Ferrocene-filled carbon nanotube peapods modified electrode	DPV	0.10 μM	0.30–100 μM	[38]
Cu_2 complex modified Au electrode	DPV	0.08 μM	0.20–30.0 μM	[39]
Flower-like Au nanostructures covered gold electrode	DPV	0.20 μM	1.00–150 μM	[40]
Nafion modified dendritic Au rod modified electrode	DPV	0.10 μM	1.00–12.0 μM	[41]
Aptamer sensor and invertase-based hydrolytic reaction	–	0.003 μM	0.08–100 μM	[42]
Molecular imprinted polymer modified glassy carbon electrode	–	0.033 μM	0.050–10.0 μM	[43]
This work		2.10 nM	5.00–300 nM	–

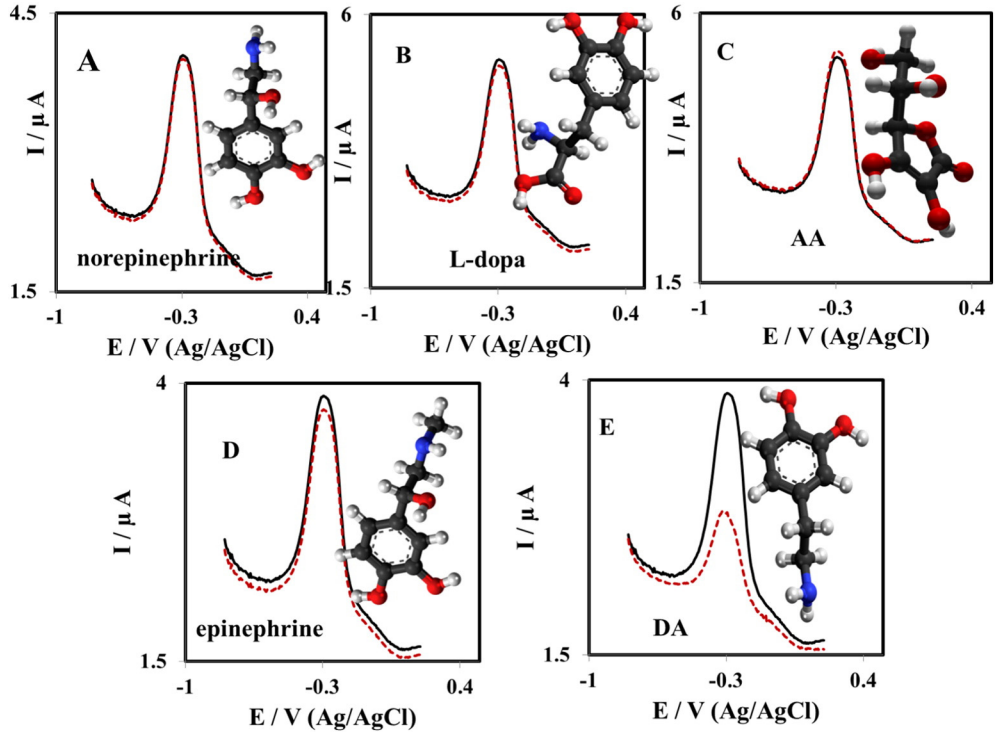

Fig. 8. DPVs of prepared aptasensor after incubating with 10 μM (A) norepinephrine, (B) L-dopa, (C) ascorbic acid (D) epinephrine, and (E) 50 nM DA in 0.1 M PBS.

variation of peak potential with scan rate, using the following Eq. (1), the charge transfer coefficient (α) was determined:

$$E_p = K - -2.3030\,(RT/\alpha nF)\log\nu \quad (1)$$

The slope of E_p vs. log (ν) was about 88 mV and the electron transferred for MB was 2, then α was calculated as 0.66. By introducing α value in the following Eq. (2), for $\Delta E_p \geq 100/n$ mV, the electron transfer rate constant was estimated to be 1.37 ± 0.03 s^{-1}.

$$\log k_s = \alpha\log(1-\alpha) + (1-\alpha)\log\alpha - \log(RT/nF\nu) - \alpha\log(1-\alpha)\,nF\Delta E/2.3RT \quad (2)$$

Furthermore, the MB redox system showed high stability. The results indicated that only 1.8% decrease in peak current of MB was observed after 100 repetitive cycles. In addition, the modified electrode response was 97% of its initial activity after it has been kept at 4 °C for 7 days. This high stability may be ascribed to the chemical and mechanical stability of the *AuNPs/PEI/CNTs-COOH* nanocomposite as well as its compatibility with the aptamer covalently attached on its surface which indicates the promising properties of *AuNPs/PEI/CNTs-COOH* as a useful platform for aptasensor fabrication. The surface coverage concentration (Γ) of MB was estimated by integrating the area under the anodic peak. According to the equation Q = Γ/nFA, the surface coverage of immobilized MB was $9.17(\pm 0.080) \times 10^{-10}$ mol cm^{-2}, indicating high loading capacity of nanocomposite for immobilization of aptamer.

3.5. Calibration modeling for DA

The aptasensor response toward DA was investigated by recording CVs of *Au/AuNPs/PEI/CNTs-COOH/aptamer/MB* modified electrode before and after incubation with 50 nM of DA (Fig. 6). As illustrated, after incubation with DA the peak current decreased due to the interaction between DA and aptamer and releasing MB from electrode surface.

In view of outstanding ability of the developed electrochemical aptasensor to sensitively detect DA, the proposed aptasensor was employed to detect different concentrations of DA (Fig.7A). Due to the higher sensitivity of DPV technique compared to the CV method, DPV was utilized for detection of DA. Good linear relationship between the MB peak current versus DA concentration in the range of 5–75 nM and 100–300 nM were observed (Fig. 7B), indicating that the DA concentration was quantitatively measured by the DPV signal.

As illustrate, two linear ranges are found; one from 5 nM to 75 nM with the regression equation of I(nA) = −0.0173[DA](nM) + 4.52 and the other from 100 to 300 nM with a regression equation of I(nA) = −0.0023[DA](nM) + 3.26. The calibration plot has a correlation coefficient of 0.996 in the range of 5–75 nM and the detection limit of 2.1 nM at signal to noise ratio of 3. Detection limit and linear calibration range of the proposed modified electrode were compared with those previously reported and the results are summarized in Table 1. As can be seen, the analytical parameters are comparable or better than the results reported for DA determination at the surface of other modified electrodes [33–43].

The reason for that the calibration curves present various linear concentration ranges with different slopes is that the amount of aptamer

Table 2
Determination of DA in human serum samples.

Sample	Added (nM)	Found (nM)	Recovery (%)
1	20.00	20.23 ± 1.01	101.1
2	40.00	38.92 ± 1.40	97.30
3	70.00	71.20 ± 1.66	101.7

immobilized on the electrode surface is some certain. When the aptasensor is used to detect DA at low concentrations, DA can readily interact with the abundant active sites of the aptamer which is immobilized on the electrode surface. At higher concentrations of DA, the active sites of the aptamer available on the aptasensor decrease. Therefore, the sensitivity declines when the aptasensor is used to determine higher concentrations of DA and calibration curves with different slopes are observed.

3.6. Selectivity of aptasensor

An excellent electrochemical aptasensor has to illustrate good selectivity. To provide the convincing evidence that the detected signal was induced by the specific interaction of the surface-confined aptamer and DA, the degree of the cross-reaction with other compound was explored under identical experimental conditions. As shown in Fig. 8, a remarkable decrease in the peak current of MB was observed by using 50 nM DA, however after incubating the aptasensor with10 μM concentration (200-fold higher than that of DA) of norepinephrine (A), L-dopa (B), ascorbic acid (C) and epinephrine (D), no recognizable signal were observed. This can be ascribed to this fact that the binding event between DA and aptamer is based on the specific recognition between them but not on the other factors, such as nonspecific adsorption. Therefore, the proposed strategy has a sufficient specificity to DA and could be identified with high selectivity.

3.7. Application of aptasensor for DA detection in in blood serum sample

To evaluate the applicability of the proposed aptasensor, the concentration of DA in human blood serum sample was determined by the standard addition method. Three blood serum samples were used and each sample analyzed three times. The detection value was the average of three results. The analytical results were shown in Table 2. The recovery was in the range 97.3–101.7%, indicating that the aptasensor had good accuracy and great potential for practical application for the analysis of DA in real clinical samples.

In order to investigate the repeatability, five repetitive measurements of 20 nM of DA solution with the proposed biosensor were used for estimating the precision of the aptasensor. According to the results, acceptable and repeatable signals with relative standard deviations (RSD) of 4.3% were obtained. Furthermore, to evaluate the reproducibility of the prepared aptasensor, four modified electrode prepared independently. The obtained RSD = 6% revealed that the aptasensor had acceptable reproducibility.

4. Conclusion

In this work, a novel nanocomposite containing polyethyleneimine (PEI)-dispersed acid-oxidized carbon nanotubes (CNTs-COOH) and AuNPs was used as a promising transduction platform to fabrication a highly sensitive DA aptasensor. ssDNA1 and ssDNA2 were attached on the surface of modified electrode using through the covalent amide bonds and hybridization, respectively. The detection limit of the aptasensor was 2.1 nM at concentration range up to 300 nM. In addition, control experiments showed that the developed aptasensor exhibited high selectivity toward DA in compared to norepinephrine, L-dopa, ascorbic acid and epinephrine. Finally, this sensor was successfully applied to DA analysis in blood serum sample. The simplicity of the fabrication procedure without using specific reagents, signal response stability and excellent sensitivity and selectivity of the aptasensor bring novel interesting applications for this sensor.

Supplementary data to this article can be found online at http://dx.doi.org/10.1016/j.msec.2016.05.077.

Acknowledgements

The authors gratefully acknowledge the support of this work by the Khorramabad Branch, Islamic Azad University for financial support.

References

[1] C. Deng, J. Chen, Z. Nie, M. Wang, X. Chu, X. Chen, X. Xiao, C. Lei, S. Yao, Impedimetric aptasensor with femtomolar sensitivity based on the enlargement of surface-charged gold nanoparticles, Anal. Chem. 81 (2009) 739–745.
[2] A. Sassolas, L.J. Blum, B.D. Leca-Bouvier, Electrochemical aptasensors, Electroanalysis 21 (2009) 1237–1250.
[3] N. Hamaguchi, A. Ellington, M. Stanton, Aptamer beacons for the direct detection of proteins, Anal. Biochem. 294 (2001) 126–131.
[4] S.S. Iqbal, M.W. Mayo, J.G. Bruno, B.V. Bronk, C.A. Batt, J.P. Chambers, A review of molecular recognition technologies for detection of biological threat agents, Biosens. Bioelectron. 15 (2000) 549–578.
[5] J. Liu, Y. Lu, Adenosine-dependent assembly of aptazyme-functionalized gold nanoparticles and its application as a colorimetric biosensor, Anal. Chem. 76 (2004) 1627–1632.
[6] S. Tombelli, M. Minunni, M. Mascini, Analytical applications of aptamers, Biosens. Bioelectron. 20 (2005) 2424–2434.
[7] C.J. Yang, S. Jockusch, M. Vicens, N. Turro, W. Tan, Light-switching excimer probes for rapid protein monitoring in complex biological fluids, Proc. Natl. Acad. Sci. 102 (2005) 17278–17283.
[8] S. Nagatoishi, Y. Tanaka, K. Tsumoto, Corrigendum to "circular dichroism spectra demonstrate formation of the thrombin-binding DNA aptamer G-quadruplex under stabilizing-cation-deficient conditions, Biochem. Biophys. Res. Commun. 352 (2007) 812–817.
[9] K.J. Feng, C. Sun, Y. Kang, J. Chen, J.H. Jiang, G.L. Shen, R.Q. Yu, Label-free electrochemical detection of nanomolar adenosine based on target-induced aptamer displacement, Electrochem. Commun. 10 (2008) 531–535.
[10] R.J. Chen, Y. Zhang, D. Wang, H. Dai, Noncovalent sidewall functionalization of single-walled carbon nanotubes for protein immobilization, J. Am. Chem. Soc. 123 (2001) 3838–3839.
[11] H. Wei, B. Li, J. Li, E. Wang, S. Dong, Simple and sensitive aptamer-based colorimetric sensing of protein using unmodified gold nanoparticle probes, Chem. Commun. 10 (2007) 3735–3737.
[12] B. Basnar, R. Elnathan, I. Willner, Following aptamer-thrombin binding by force measurements, Anal. Chem. 78 (2006) 3638–3642.
[13] Y. Li, H.J. Lee, R.M. Corn, Fabrication and characterization of RNA aptamer microarrays for the study of protein–aptamer interactions with SPR imaging, Nucleic Acids Res. 34 (2006) 6416–6424.
[14] W. Cheng, S.J. Ding, Q. Li, T.X. Yu, Y.B. Yin, H.X. Ju, G.S. Ren, A simple electrochemical aptasensor for ultrasensitive protein detection using cyclic target-induced primer extension, Biosens. Bioelectron. 36 (2012) 12–17.
[15] X.L. Zuo, Y. Xiao, K.W. Plaxco, High specificity, electrochemical sandwich assays based on single aptamer sequences and suitable for the direct detection of small-molecule targets in blood and other complex matrices, J. Am. Chem. Soc. 131 (2009) 6944–6945.
[16] X. Sun, F.L. Li, G.H. Shen, J.D. Huang, X.Y. Wang, Aptasensor based on the synergistic contributions of chitosan–gold nanoparticles, graphene–gold nanoparticles and multi-walled carbon nanotubes-cobalt phthalocyanine nanocomposites for kanamycin detection, Analyst 139 (2014) 299–308.
[17] Q.L. Xu, J.Y. Yoon, Visual detection of dopamine and monitoring tyrosinase activity using a pyrocatechol violet-Sn^{4+} complex, Chem. Commun. 47 (2011) 12497–12499.
[18] E. Farjami, R. Campos, J.S. Nielsen, K.V. Gothelf, J. Kjems, E.E. Ferapontova, RNA aptamer-based electrochemical biosensor for selective and label-free analysis of dopamine, Anal. Chem. 85 (2013) 121–128.
[19] T. Qian, S.S. Wu, J. Shen, Facilely prepared polypyrrole-reduced graphite oxide core–shell microspheres with high dispersibility for electrochemical detection of dopamine, Chem. Commun. 49 (2013) 4610–4612.
[20] L. Sasso, A. Heiskanen, F. Diazzi, M. Dimaki, J. Castillo-Leon, M. Vergani, E. Landini, R. Raiteri, G. Ferrari, M. Carminati, M. Sampietro, W.E. Svendsen, J. Emneus, Doped overoxidized polypyrrole microelectrodes as sensors for the detection of dopamine released from cell populations, Analyst 138 (2013) 3651–3659.
[21] G. Fabregat, F. Estrany, M.T. Casas, C. Aleman, E. Armelin, Detection of dopamine using chemically synthesized multilayered hollow microspheres, J. Phys. Chem. B 118 (2014) 4702–4709.
[22] R. Walsh, M.C.D. Rosa, Retention of function in the DNA homolog of the RNA dopamine aptamer, Biochem. Biophys. Res. Commun. 388 (2009) 732–735.
[23] Q. Mu, H. Xu, Y. Li, S.J. Ma, X.H. Zhong, Adenosine capped QDs based fluorescent sensor for detection of dopamine with high selectivity and sensitivity, Analyst 139 (2014) 93–98.
[24] S. Liu, X.R. Xing, J.H. Yu, W.J. Lian, J. Li, M. Cui, J.D. Huang, A novel label free electrochemical aptasensor based on graphene–polyaniline composite film for dopamine determination, Biosens. Bioelectron. 36 (2012) 186–191.
[25] L. Zhang, Y. Cheng, J.P. Lei, Y.T. Liu, Q. Hao, H.X. Ju, Stepwise chemical reaction strategy for highly sensitive electrochemiluminescent detection of dopamine, Anal. Chem. 85 (2013) 8001–8007.
[26] X. Hu, T. Wang, X. Qu, S. Dong, In situ synthesis and characterization of multi-walled carbon nanotube/Au nanoparticle composite materials, J. Phys. Chem. B 110 (2006) 853–857.

[27] L. Jin, X. Gao, L. Wang, Q. Wu, Z. Chen, X. Lin, Electrochemical activation of polyethyleneimine-wrapped carbon nanotubes/in situ formed gold nanoparticles functionalised nanocomposite sensor for high sensitive and selective determination of dopamine, J. Electroanal. Chem. 692 (2013) 1–8.
[28] E. Munoz, D.S. Suh, S. Collins, M. Selvidge, A.B. Dalton, B.G. Kim, J.M. Razal, G. Ussery, A.G. Rinzler, M.T. Martnez, R.H. Baughman, Highly conducting carbonnanotube/polyethyleneimine composite fibers, Adv. Mater. 17 (2005) 1064–1068.
[29] X. Feng, C. Mao, G. Yang, W. Hou, J. Zhu, Polyaniline/Au composite hollow spheres: synthesis, characterization and application to the detection of dopamine, Langmuir 22 (2006) 4384–4389.
[30] J.J. Sun, H.Z. Zhao, Q.Z. Yang, J. Song, A. Xue, A novel layer-by-layer self-assembled carbon nanotube-based anode: preparation, characterization and application in microbial fuel cell, Electrochim. Acta 55 (2010) 3041–3047.
[31] M. Shen, S.H. Wang, X. Shi, X. Chen, Q. Huang, E.J. Petersen, R.A. Pinto, J.R. Baker Jr., W.J. Weber Jr., Polyethyleneimine mediated functionalization of multiwalled carbon nanotubes: synthesis, characterization and in vitro toxicity assay, J. Phys. Chem. C 113 (2009) 3150–3156.
[32] E. Laviron, General expression of the linear potential sweep voltammogram in the case of diffusionless electrochemical systems, J. Electroanal. Chem. 101 (1979) 19–28.
[33] T.A. Mir, M.H. Akhtar, N.G. Gurudatt, J.I. Kim, C.S. Choi, Y.B. Shim, An amperometric nanobiosensor for the selective detection of K-induced dopamine released from living cells, Biosens. Bioelectron. 68 (2015) 421–428.
[34] X.F. Gu, G.M. Jiang, G.Q. Jiang, T.T. Chen, W.Y. Zhan, X. Li, Detection of dopamine on a mercaptoterminated hexanuclear Fe(III) cluster modified gold electrode, Talanta 137 (2015) 189–196.
[35] P. Si, H.L. Chen, P. Kannan, D. Kim, Selective and sensitive determination of dopamine by composites of polypyrrole and graphene modified electrodes, Analyst 136 (2011) 5134–5138.
[36] G. Fabregat, F. Estrany, M.T. Casas, C. Aleman, E. Armelin, Detection of dopamine using chemically synthesized multilayered hollow microspheres, J. Phys. Chem. B 118 (2014) 4702–4709.
[37] Q.M. Feng, M. Cai, C.G. Shi, N. Bao, H.Y. Gu, Integrated paper-based electroanalytical devices for determination of dopamine extracted from striatum of rat, Sensors Actuators B 209 (2015) 870–876.
[38] H.M. Cheng, L.H. Guan, Z.J. Shi, Z.W. Zhu, Z.N. Gu, M. Li, Bi-directional electrocatalytic detection of dopamine at an electrode modified with ferrocene filled carbon nanotube peapods, Electroanalysis 25 (2013) 2041–2044.
[39] G.M. Jiang, X.F. Gu, G.Q. Jiang, T.T. Chen, W.Y. Zhan, S. Tian, Application of a mercaptoterminated binuclear Cu(II) complex modified Au electrode to improve the sensitivity and selectivity for dopamine detection, Sensors Actuators B 209 (2015) 122–130.
[40] H. Beitollahi, M. Mazloum-Ardakani, B. Ganjipour, H. Naeimi, Novel 2,2′- [1,2 ethanediylbis (nitriloethylidyne)]-bis-hydroquinone double-wall carbon nanotube paste electrode for simultaneous determination of epinephrine, uric acid and folic acid, Biosens. Bioelectron. 24 (2008) 362–368.
[41] Y. Zhao, S.H. Li, J. Chu, Y.P. Chen, W.W. Li, H.Q. Liu, Y.C. Tian, Y. Xiong, A nano-sized Au electrode fabricated using lithographic technology for electrochemical detection of dopamine, Biosens. Bioelectron. 35 (2012) 115–122.
[42] X. Hun, Y. Xu, G. Xie, X. Luo, Aptamer biosensor for highly sensitive and selective detection of dopamine using ubiquitous personal glucose meters, Sensors Actuators B 209 (2015) 596–601.
[43] M. Zhong, Y. Teng, S.F. Pang, L.Q. Yan, X.W. Kan, Pyrrole-phenylboronic acid: a novel monomer for dopamine recognition and detection based on imprinted electrochemical sensor, Biosens. Bioelectron. 64 (2015) 212–218.